



Article

Optimization of Sintering Process of Alumina Ceramics Using Response Surface Methodology

Darko Landek ^{1,*}, Lidija Ćurković ^{1,*} , Ivana Gabelica ¹, Mihone Kerolli Mustafa ² and Irena Žmak ¹ 

¹ Department of Materials, Faculty of Mechanical Engineering and Naval Architecture, University of Zagreb, Ivana Lučića 5, 10000 Zagreb, Croatia; ivana.gabelica@fsb.hr (I.G.); irena.zmak@fsb.hr (I.Ž.)

² International Business College Mitrovica, Str. Bislim Bajgora nn, 40000 Mitrovica, Kosovo; m.kerolli@ibcmitrovica.eu

* Correspondence: darko.landek@fsb.hr (D.L.); lidija.curkovic@fsb.hr (L.Ć.); Tel.: +385-1-616-8353 (D.L.); +385-1-616-8183 (L.Ć.)

Abstract: In this work, alumina (Al₂O₃) ceramics were prepared using an environmentally friendly slip casting method. To this end, highly concentrated (70 wt.%) aqueous suspensions of alumina (Al₂O₃) were prepared with different amounts of the ammonium salt of a polycarboxylic acid, Dolapix CE 64, as an electrosteric dispersant. The stability of highly concentrated Al₂O₃ aqueous suspensions was monitored by viscosity measurements. Green bodies (ceramics before sintering) were obtained by pouring the stable Al₂O₃ aqueous suspensions into dry porous plaster molds. The obtained Al₂O₃ ceramic green bodies were sintered in the electric furnace. Analysis of the effect of three sintering parameters (sintering temperature, heating rate and holding time) on the density of alumina ceramics was performed using the response surface methodology (RSM), based on experimental data obtained according to Box–Behnken experimental design, using the software Design-Expert. From the statistical analysis, linear and nonlinear models with added first-order interaction were developed for prediction and optimization of density-dependent variables: sintering temperature, heating rate and holding time.

Keywords: alumina; slip casting; sintering; Box–Behnken design; response surface method



Citation: Landek, D.; Ćurković, L.; Gabelica, I.; Kerolli Mustafa, M.; Žmak, I. Optimization of Sintering Process of Alumina Ceramics Using Response Surface Methodology. *Sustainability* **2021**, *13*, 6739. <https://doi.org/10.3390/su13126739>

Academic Editors: Lin Li, Karl R. Haapala, Sophie I. Hallstedt and Yiran (Emma) Yang

Received: 8 May 2021
Accepted: 12 June 2021
Published: 14 June 2021

Publisher's Note: MDPI stays neutral with regard to jurisdictional claims in published maps and institutional affiliations.



Copyright: © 2021 by the authors. Licensee MDPI, Basel, Switzerland. This article is an open access article distributed under the terms and conditions of the Creative Commons Attribution (CC BY) license (<https://creativecommons.org/licenses/by/4.0/>).

1. Introduction

Alumina is an important raw material in the global advanced ceramics industry because of three key advantages compared to other ceramics [1]: (i) it has an industrially high usable combination of mechanical, tribological and dielectric properties and chemical inertness [2]; (ii) raw alumina is an inexpensive and easily available material [3]; and (iii) it can be shaped and sintered to full density in air atmosphere. Similar to other engineering ceramics, slip casting alumina products are formed in three steps: preparation of a stable suspension, formation of the green body (ceramic before sintering) and green body densification by sintering. Currently, a lot of effort is put into the development of low-cost forming and sintering technologies for complex ceramic components. The following main shaping processes before sintering are actually in the stage of commercialization or development: slip casting, freeze casting, tape casting/lamination, powder injection molding, extrusion, cold isostatic pressing, uniaxial die pressing, additive manufacturing and colloidal processing of powders [1,2]. Colloidal shaping methods enable achievement of high microstructural homogeneity in green and sintered parts and offer near-net shaping capabilities that reduce post-sintering machining and production costs.

Slip casting as a colloidal shaping method is one of the most common forming techniques, used in the commercial production of different advanced ceramics. The first phase in the slip casting process is the preparation of stable concentrated aqueous suspensions of the ceramic powders mixed with dispersants and binders. At high solid loading, relatively low slip viscosity can only be achieved in the presence of an optimum dispersion state of

particles. The second phase is casting suspension into a plaster mold and drying it until a steadily green body is obtained. The described procedure is simple, reliable, flexible, cost-effective and pollution-free, but it requires an adequate understanding of colloid suspensions and their behavior. This knowledge is crucial for the optimization of the amount of used dispersant, binder and an agent for preventing abnormal grain growth. While there are many commercially available dispersants and binders, only a specific combination of dispersant/binder can be used with the starting powder size for optimal slip casting of alumina ceramics [3].

The size of powder particles, the method of preparing a dispersed solution and casting and drying of the ceramic slurry are of crucial influence for the optimum performance of the sintering process and ceramic product properties. When powder particles are nano size, the sintering is better and, consequently, product properties are better, too. On the other hand, particles smaller than 1 μm , in a combination with high suspension concentration, increase the suspension viscosity [4,5]. Strong interactions among particles can lead to agglomeration or flocculation [6,7]. This interaction can be controlled with chemical additives in three different ways: electrostatic, steric and electrosteric stabilization [8–10]. The selection of dispersant is a critical step in slurry preparation because it might be difficult to find a dispersant that is optimal for all suspension components and for establishing control over the suspension stability and its rheological properties [11,12]. To select the optimal suspension dispersant, it is recommended to conduct preliminary viscosity measurements and sedimentation tests with the variation of type and content of dispersants and binders. The highly concentrated alumina suspensions show non-Newtonian dependence of shear stress on viscosity for which three rheological models have been proposed and tested: the power law, the Herschel–Bulkley fluid and the Bingham plastic model [10,13].

The solid-state sintering presents the third step in ceramics production. For alumina ceramic, solid-state sintering involves densifying a green body into a dense solid object at a high temperature above 1500–1800 °C without melting (the melting point of alumina is 2050 °C). Sintering to full density can be achieved at atmospheric pressure (pressureless sintering). The methods for heat supply in pressureless sintering can be conventional slow heating in an electrical or vacuum furnace with or without inert atmosphere [1,14,15], or rapid heating in a microwave furnace [16,17] and heating by plasma in spark plasma sintering [18]. Solid-state sintering is correlated with many factors: particle size, green body density, the occurrence of agglomerates, sintering temperature, holding time, heating rate, cooling rate [1,14,15,19] etc. The most influential parameters on solid-body density and properties are initial grain size, sintering temperature and time. Decreasing initial grain size increases sintering rate and reduces required holding time. The effect of initial grain size on holding time is explained by Herring's scaling law. For the sintering of two ceramics with different average radii of grains r_1 and r_2 , where $r_2 = \lambda r_1$ ($\lambda > 1$), the required holding times t_2 and t_1 are interconnected by the relation $t_2 = \lambda^\alpha t_1$. The exponent α depends on sintering mechanisms and can assume value from 1 to 4 [20]. The strong effect of increasing temperature on increasing sintering rate arises from the fact that sintering is a thermally activated process in which variables such as diffusivity, viscosity, etc., are expressed as exponential functions of temperature. On the other hand, increased sintering temperature promoted grain growth and weaker mechanical properties [15,19]. The holding time has a smaller impact on the properties of sintered ceramics in relation to the sintering temperature. In kinetic equations for various mechanisms of sintering the natural logarithm of holding time $\ln(t)$ is proportional to the inverse value of the sintering temperature ($1/T$), to achieve the same degree of sintering [20].

For the preparation of the optimal sintering process, the optimal viscosity of the suspension and optimal combination of sintering parameters should be obtained, which will give the highest workpiece density, fine-grained structure, highest toughness, flexural strength, hardness etc. In search of the optimal combination of sintering parameters, their individual and joint action on the properties of the sintered product should be taken into

account. Such a possibility is provided by the application of design of experiments (DOE) and statistical analysis of experimental results.

Experimental data from sintering processes are analyzed using various methods. One of these, response surface methodology (RSM), is used in this work, in combination with analysis of variance (ANOVA). RSM is a frequently used method for modelling. For example, Batista et al. modelled the combustion process of hydroxyapatite [21], Khajelakzay et al. applied RSM to optimize the spark plasma sintering process for the fabrication of $\text{Si}_3\text{N}_4\text{-SiC/MgSiN}_2$ [22], Das et al. improved the tribological properties of glass-ceramics using RSM to model the output responses [23]. To determine the operational conditions for preparing magnesia partially stabilized zirconia refractory, Jiang et al. used RSM [24]. Arzani et al. used RSM based on the central composite design (CCD) to analyze operating parameters for the preparation of mullite ceramic microfilter membranes [25]. Kockal et al. used RSM to optimize the response of input variables to produce a ceramic tile with improved properties [26].

In this paper, two effects were investigated: (i) the impact of dispersant Dolapix CE 64 on the viscosity of an aqueous suspension for slip casting to achieve the minimum viscosity for good mold filling, and (ii) the influence of the basic sintering parameters (temperature, heating rate and holding time) on the density of alumina ceramic samples' conventional sintering in the electrically heated furnace. The influence of sintering parameters was analyzed by RSM and regression analysis with the aim to develop a new regression model which will include individual and joint influences of sintering parameters on the density of conventionally sintered aluminum oxide ceramics.

2. Materials and Methods

2.1. Suspension Preparation

Aqueous alumina suspensions with a solid loading of 70 wt.% were prepared from high purity Al_2O_3 powder with average particle size of 300–400 nm (Alcan Chemicals, Stamford, CT, USA), dispersant Dolapix CE 64 (Zschimmer & Schwarz GmbH & Co KG, Chemische Fabriken, Lahnstein, Germany) and deionized water. The dispersant Dolapix CE 64 is 70 wt.% aqueous solution of the ammonium salt of polymethacrylic acid (PMAA- NH_4). The amount of Dolapix CE 64 was varied to determine its optimal content, which is reflected in the obtained minimal viscosity. The dispersant contents were: 0.15, 0.2, 0.4, 0.6, 0.8 and 1.0 wt.%, based on the amount of dry ceramic powder. According to preliminary results, it was found that the optimal pH value of alumina suspension is 10. Therefore, the pH value of all suspensions was set to 10 by the addition of 1 M NaOH aqueous solution. All suspensions were prepared by adding deionized water, containing dissolved Dolapix CE 64 and ceramic powder at the set pH value of 10. The prepared suspension was put into the grinding jar of a planetary ball mill. The grinding jar and ten balls used for homogenization are made of alumina ceramics to prevent the contamination of suspensions. Each of the prepared suspensions was homogenized for 90 min at a rate of 300 rpm in the planetary ball mill (PM 100, Retsch, Germany). To remove air bubbles and to achieve better homogeneity of prepared suspensions, each of them was treated in an ultrasonic bath.

2.2. Determination of Rheological Properties and Density

After homogenization, all alumina suspensions were subjected to rheological measurements, one at a time. A volume of 8 cm^3 of each prepared suspension was used to measure the rheological properties on the rotational viscometer Brookfield DV-III Ultra, USA, with accompanying software Rheocalc. The testing temperature was held constant at $25 \pm 1^\circ\text{C}$. To avoid the influence of all previous occurrences ("sample history") on the results, each suspension was subjected to pre-shearing at the shear rate of 100 s^{-1} for 2 min. Subsequently, flow curves were recorded to show the dependence of the shear stress and viscosity on the shear rate. The shear rate, $\dot{\gamma}$, was increased from 0 s^{-1} to 180 s^{-1} with 50 equal intervals, which lasted for 3 s. Measurements were made just before each rate change.

Based on previous studies of rheological properties of concentrated alumina suspensions with the addition of the dispersant Dolapix CE 64 [12,13], a shear rate γ , of 50 s^{-1} was chosen to enable minimal viscosity for slip casting process. This shear rate was held constant during all gravity slip casting experiments. Sample density was determined by the Archimedean method using the Mettler Toledo JP703C analytical balance. All experiments were carried out under ambient laboratory conditions.

2.3. Design of Solid-State Sintering Experiments

The prepared stable high concentrated alumina suspensions with the optimal amount of dispersant Dolapix CE 64 were cast in gypsum molds ($20 \text{ mm} \times 20 \text{ mm} \times 20 \text{ mm}$) to prepare the green bodies. The obtained green bodies were sintered in the electrical furnace based on the Box–Behnken test plan (33 factorial design) [12,15] with the variation of three independent variables: sintering temperature (A), heating rate (B) and holding time (C), with variations over three levels: high (+1), low (−1) and the center points (coded level 0). The sintering factors and levels involved in the experiments are summarized in Table 1. The response variable is sintered-body density (ρ , g/cm^3). The analysis of results was conducted with the response surface method (RSM) [21], using the Design-Expert software. The experimental design applied significantly simplifies the test because, instead of a maximum of 27 experiments, only 17 experiments with 13 different conditions need to be performed to construct a response surface, with the repetition of the condition at the central point of the experiment 5 times. For each combination of sintering parameters, three castings were fabricated, and the density was measured after pressureless sintering in the electric furnace in an air atmosphere.

Table 1. Independent variables and their levels in the experimental design.

Symbol	Factors	Levels		
		−1	0	1
A	Sintering temperature ($^{\circ}\text{C}$)	1600	1625	1650
B	Heating rate ($^{\circ}\text{C}/\text{min}$)	3	5	7
C	Holding time (h)	2	4	7

3. Results and Discussion

3.1. Rheological Measurements of Suspensions Viscosity

Rheological measurements were used to determine the optimal dispersant amount in 70 wt.% alumina suspensions, which is in correlation with the lowest achieved viscosity at the shear rate of 50 s^{-1} . It is the exact shear rate that can be repeatably and easily reached in gravity slip casting. Figure 1 shows the results of testing the effect of the dispersant content on the viscosity of the suspension. It can be observed that the lowest viscosity is not joined to the highest amount of the dispersant, but for the “optimal” amount, which is 0.2 wt.% of the dry powder content. The average dynamic viscosity for that composition was 7.06 mPas.

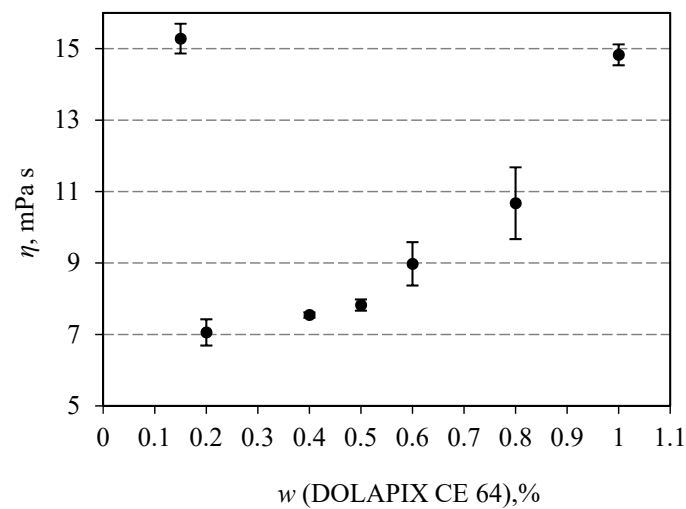


Figure 1. The dependence of viscosity on the concentration of Dolapix CE 64 for the investigated Al_2O_3 suspensions, pH value of all suspensions was 10.

Qualitatively similar behavior was observed in independent works [3,7,9] with dispersants Duramax, Darvan C and Dolapix CE at high concentrations of Al_2O_3 powder in suspension, over 70% wt.

This behavior can be explained by the Dolapix CE 64 electrosteric contribution to the stabilization of alumina suspension and preventing direct contact between particles [27,28]. In the Al_2O_3 suspension, the molecules of the dispersant Dolapix CE 64 are anchored to the surface of the ceramic particles by the hydrophobic part, and by the hydrophilic part, they are directed into the suspension. In this way, they create electric potential around Al_2O_3 particles and cause the repulsion of adjacent particles. For the low concentrations of the Dolapix CE 64, the long ranged repulsive electrostatic forces between double layers around the alumina particles hold the main role in increasing suspension viscosity. With increasing concentrations of the Dolapix CE 64 up to 0.2 wt.% more surface area of Al_2O_3 particles was covered by the electrosteric molecules, and the steric forces lubricate the particle contacts and hinder particle coagulation. Increasing the content of Dolapix CE 64 above 0.5 wt.% leads to an increase in the thickness of the electrically charged layer around Al_2O_3 particles and to a greater number of collisions of hydrophilic parts of the dispersant molecules. Both of these phenomena cause coagulation of the particles and increase the viscosity of the suspension.

3.2. Analysis of Sintering Density with the Response Surface Method

All samples for sintering experiments were made from the same aqueous suspension with Al_2O_3 powder content of 70 wt.% and by the addition of 0.2 wt.% of Dolapix CE 64. The mean density values of sintered Al_2O_3 ceramics tested for individual sintering parameters are shown in Table 2. The measured density values are in the range of 3.833 g/cm^3 – 3.893 g/cm^3 . The theoretical density of pure Al_2O_3 is 3.97 g/cm^3 . From the theoretical density value of pure alumina ceramics and the measured bulk densities, the calculated relative densities of each sample were from 96.55% to 98.06%. It can be observed that the range of density values of sintered aluminum oxide ceramics is very small, $\Delta\rho = 0.060 \text{ g/cm}^3$. In the Design-Expert software, a linear correlation of the density and each sintering parameter into the assumed linear regression model was examined.

Table 2. Experimental design and results of the Box–Behnken design.

Run	Factor A	Factor B	Factor C	ρ
	Sintering Temperature, °C	Heating Rate, °C/min	Holding Time, h	Density, g/cm ³
1	1650	5	2	3.841 ± 0.0297
2	1600	7	4	3.836 ± 0.0267
3	1625	3	6	3.891 ± 0.0074
4	1625	7	6	3.893 ± 0.0040
5	1625	5	4	3.885 ± 0.0086
6	1600	3	4	3.854 ± 0.0316
7	1650	7	4	3.887 ± 0.0095
8	1650	5	6	3.887 ± 0.0046
9	1600	5	2	3.879 ± 0.0032
10	1600	5	6	3.869 ± 0.0012
11	1625	7	2	3.844 ± 0.0036
12	1650	3	4	3.885 ± 0.0040
13	1625	3	2	3.833 ± 0.0103

Most ceramic materials shrink during sintering, i.e., the sample dimensions are reduced. Linear shrinkage is calculated as the percentage change in dimension of green body during sintering, according to the following equation:

$$\Delta x = \left| \frac{x_2 - x_1}{x_1} \right| \cdot 100 \quad (1)$$

where:

Δx —linear shrinkage, %,

x_1 —dimension of green body samples before sintering, mm,

x_2 —dimension of sintered ceramics samples, mm.

Linear and isotropic shrinkage of sintered alumina ceramics was from 9.30% to 10.20%.

Figure 2A shows the density dependence of Al₂O₃ ceramics (y-axis) on sintering temperature (x-axis). From results in Figure 2A a correlation coefficient $r_{AD} = -0.054$ is calculated. Therefore, it can be concluded that in the sintering temperature range from 1600 °C to 1650 °C, the mean density value is not significantly dependent of the temperature increase. The same conclusion is valid for the correlation between density and heating rate shown in Figure 2B, where a correlation coefficient of $r_{BD} = -0.008$ is calculated. It can be concluded that in the observed interval of sintering temperature the achieved density of Al₂O₃ ceramics almost does not significantly depend on the heating rate. Figure 2C shows the density values of Al₂O₃ ceramics' (y-axis) dependence on the holding time at constant sintering temperature (x-axis). A linear correlation coefficient $r_{CD} = 0.580$ was calculated. Therefore, it is possible to conclude that the linear correlation of these two variables is of medium strength. With a longer holding time at the sintering temperature, the dissipation of the density of Al₂O₃ ceramics decreases.

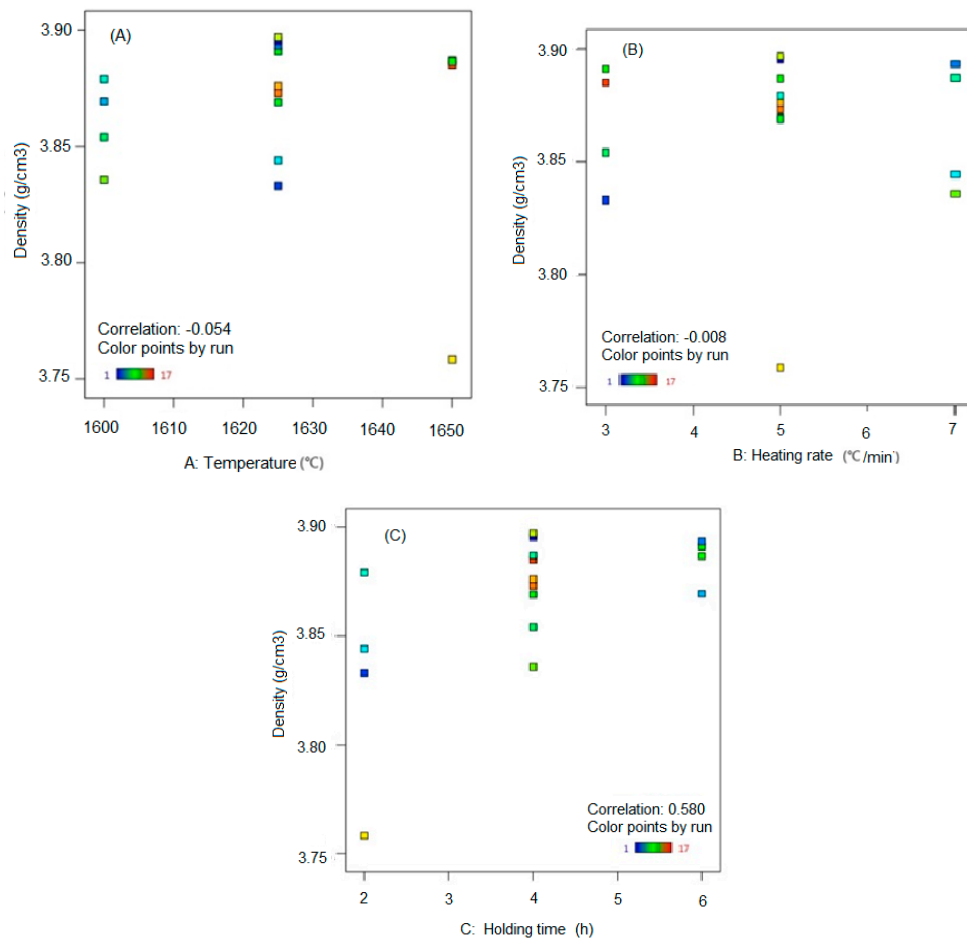


Figure 2. Linear correlation between Al_2O_3 ceramic density and: (A) sintering temperature, (B) heating rate, and (C) holding time.

Figure 3 shows a 3D representation of the combined effect of all independent variables on the density of Al_2O_3 ceramics, with measured values from 17 runs. Figure 3A–C show the density dependence on the heating rate and sintering temperature at a constant sintering time in the duration of 2 h, 4 h and 6 h. The expected amount of Al_2O_3 ceramic density is almost independent of the heating rate when varying the heating rate and sintering temperature. The shape of the surface does not change with the change of the constant holding duration parameter, only the slope in space changes.

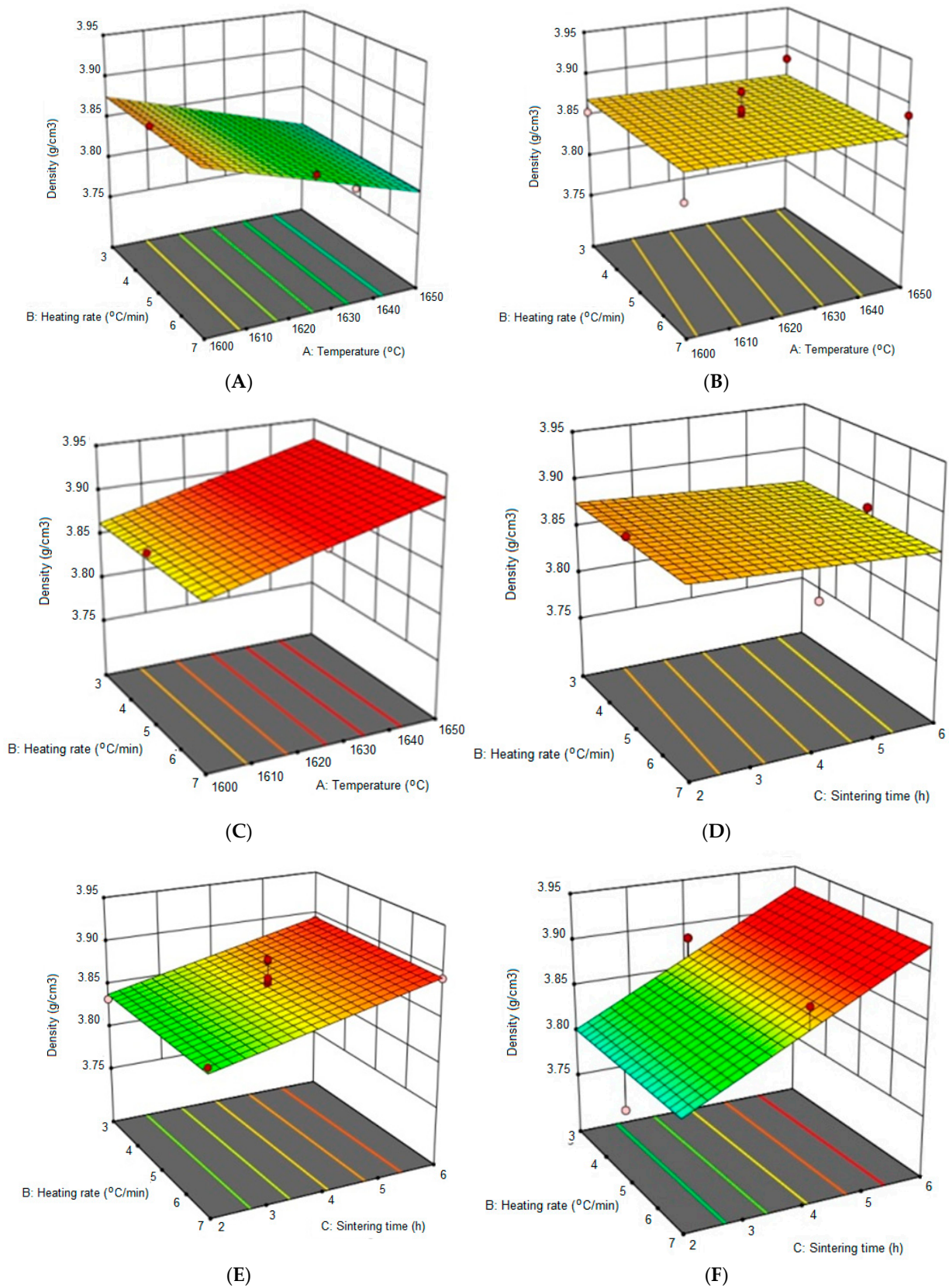


Figure 3. The 3D response graphs, the effect of sintering temperature, holding time and heating rate on Al₂O₃ density. Holding time of (A) 2 h, (B) 4 h and (C) 6 h; sintering temperature of (D) 1600 °C, (E) 1625 °C and (F) 1650 °C.

Figure 3D–F show the dependence of the density on the heating rate and the sintering time for sintering temperatures of 1600 °C, 1625 °C and 1650 °C. From these graphs, it can be seen that the density of Al₂O₃ ceramics changes concerning the holding time. The density increases linearly with the increase in the holding time, for sintering temperatures above 1600 °C. As the sintering temperature increases, the slope of the response surface is higher and suggests a stronger influence of the holding time on the density of sintered Al₂O₃ ceramics. According to the results, the heating rate does not significantly affect the density of Al₂O₃ ceramics.

Figure 4 shows a 3D representation of the combined effects of sintering temperature and sintering time on the density of Al₂O₃ ceramics. The maximum density of Al₂O₃ ceramics is achieved at the highest sintering temperature and the longest holding time. Minimum sample density is achieved in two cases: (1) at the highest sintering temperature and the shortest holding time, (2) at the lowest sintering temperature and the longest holding time. Therefore, the response surface of the density-dependence on the sintering temperature and holding time involves a saddle and indicates the significance of the joint effect of temperature and time on the density of sintered Al₂O₃ ceramics.

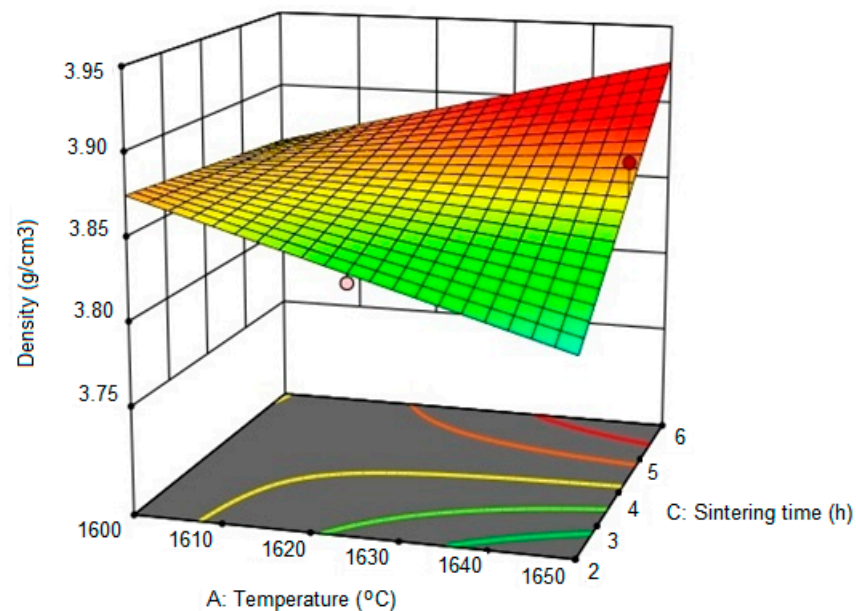


Figure 4. 3D representation of the relationship between the density of Al₂O₃ ceramics, temperature and holding time at the sintering temperature, for the heating rate of 7 °C/min.

Figure 5 shows the influence of individual factors (A-sintering temperature, B-heating rate, C-holding time) on the increase of the estimated model variance. The view shows that the precision at the center of the experiment is excellent (the estimation of model variance is 0.45), but the precision drops according to the lower and upper level of the individual factors (the estimation of model variance is 0.60).

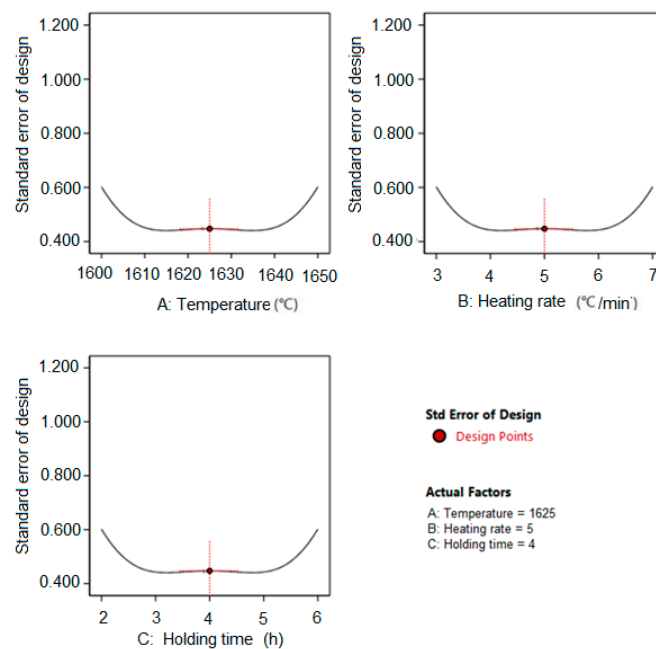


Figure 5. Increase in the estimated variance with respect to the value of individual parameters.

With the results of the experiments from Table 2, a three-factor analysis of variance (ANOVA) was performed at three levels with the assumption of linear, quadratic, and modified linear models with added first-order interactions. For the chosen regression model to be significant, the p -value of the category “Model” should be less than 0.05, and the p -value of the category “Lack of Fit” should be greater than 0.05. The p -value for the category “Lack of Fit” compares the residual error to the “pure error” from replicated experimental design points. When this p -value is greater than 0.05, the lack of fit for the selected model becomes insignificant and the model is acceptable [29]. With the test results from Table 2, the RSM analysis was performed, using linear and quadratic models with and without adding factors (see Table 1, A-sintering temperature, B-heating rate, C-holding time) and with adding and subtracting interactions of all tested factors: AB, BC, ABC, AA, BB, CC. For further analysis, two RSM models with one interaction were proposed: a linear model in the form $D = f(A, B, C, AC)$ and a nonlinear model with modified independent variables in the form $D = f(A', C', A'C')$.

3.3. Linear RSM Model with One Interaction

Based on ANOVA analysis, a linear model with the first-order interaction was proposed and expressed with Equation (2).

$$\rho = 8.46634 - 0.002865 \times T - 0.000187 \times v_h - 1.10713 \times t_s + 0.00069 \times T \times t_s \quad (2)$$

where:

ρ -is density of sintered alumina, g/cm³

T -sintering temperature, °C

v_h -heating rate, °C/min

t_s -holding time, h

The results of the ANOVA for the selected linear model with interaction are shown in Table 3.

Table 3. Analysis of variance for response surface in the linear model of Al₂O₃ density conducted by the Design-Expert software (DF-Degrees of Freedom).

Source of Variations	Sum of Squares	DF	Mean Square	F-Value	p-Value	p < 0.05
Model	0.0112	4	0.0028	4.3100	0.0216	Significant
A: Temperature	0.0001	1	0.0001	0.0849	0.7757	
B: Heating rate	1.13×10^{-6}	1	1.13×10^{-6}	0.0017	0.9675	
C: Holding time	0.0064	1	0.0064	9.8300	0.0086	
Interaction AC	0.0048	1	0.0048	7.3300	0.0190	
Residual	0.0078	12	0.0006			
Lack of Fit	0.0071	8	0.0009	5.1400	0.0655	Not significant
Pure Error	0.0007	4	0.00017			
Cor Total	0.0189	16				

The selected linear model has a p -value of 0.0216, significantly lower than 0.05, and the p -value for the “lack of fit” category is 0.0655 which is greater than 0.05. According to the ANOVA results, the most significant factor of the three observed was the holding time (C) at the sintering temperature (A). Temperature and heating rate do not have a significant effect on the response or density. Therefore, only the interaction of the factor, sintering temperature factor and holding time (AC) factor was used in the selected model. The other two interactions (AB and BC) were excluded due to low p -values, and their influence on the response variable was not statistically significant. The linear RSM model in Equation (2) has a low coefficient determination $R^2 = 0.475$. The obtained value of the coefficient R^2 indicates a larger error in predicting the density of sintered ceramics using Equation (2) thus limiting its application.

3.4. Nonlinear RSM Model with One Interaction

Since the Box–Behnken method is not suitable for the development of cubic and higher-order models, besides a linear model (2) with added first-order interactions, it is possible to set up a nonlinear quadratic model. For this model an RSM analysis was performed with modified factors A' , B' , and C' based on the following consideration. Ceramic sintering is a thermally activated diffusion process in which the rate of the diffusion process (k) is temperature-dependent according to the Arrhenius law ($k = k_0 \exp(-Q/RT)$), where k_0 is a constant, Q is activation energy and T is temperature. Increasing the diffusion rate increases the flow of atoms in the grain and necks between the sintered grains, which leads to a decrease in the porosity between the grains, and in turn to an increase in the density of the sintered ceramic. In the logarithmic notation of the Arrhenius law, the speed of a thermally activated process (k) is inversely proportional to the temperature at which the process is carried out. From this consideration follows the assumption that in the RSM model for predicting the density of sintered ceramics, the independent variable A is included in a modified form $A' = 1/A$. The influence of the heating rate on the density of the sintered ceramics proved to be statistically insignificant and will be ignored by the proposed nonlinear model. The influence of holding time on sintering density was assumed to be in the form $C' = 1/\sqrt{C}$. The assumed dependence follows from the fact that the thickness (d_g) of the new layer of atoms on crystal grains in thermally activated processes is proportional to the growth rate of the layer (k_g) and the square root of time (t), which is expressed by the empirical equation: $d_g = k_g \sqrt{t}$. It follows from this equation that the growth rate of the layer is inversely proportional to the square root of the growth time of the layer: $k_g = d_g / \sqrt{t}$. The increases in the growth rate of the new layer (k_g), between the sintered grains, together with increasing the diffusion rate (k) increase the sintering density (response variable D of the RSM model). Based on these facts, the proposed nonlinear RSM model is analyzed in the form $D = f(A', C', A'C')$ and expressed with Equation (3). The coefficient of determination for the model (3) is $R^2 = 0.678$.

$$\rho = 9.3 - 10161 \times (T + 273.15)^{-1} - 9.1 \times (\sqrt{t_s})^{-1} + 17097.1 \times (T + 273.15)^{-1} \times (\sqrt{t_s})^{-1} \quad (3)$$

The meaning and units of measurement for variables in Equation (3) are the same as in Equation (2). Results of ANOVA for the model given by Equation (3) are shown in Table 4. According to the results of ANOVA (Table 4), the nonlinear model (3) more reliably predicts the density of sintered ceramics than the linear model (2) and is composed of only the two most influential factors, sintering temperature (T) and holding time (t_s). Both factors and their interaction are statistically significant, and they have p -value below 0.05. The lack of fit value of the nonlinear model (3) is greater than 0.05 similarly as with the linear model (2).

Table 4. Analysis of variance for response surface in the nonlinear model of Al_2O_3 density conducted by the Design-Expert software (DF-Degrees of Freedom).

Source of Variations	Sum of Squares	DF	Mean Square	F-Value	p -Value	$p < 0.05$
Model	0.0043	3	0.00148	6.580	0.012	Significant
A' : Temperature	0.0030	1	0.00300	2.727	0.023	Significant
C' : Holding time	0.0004	1	0.00089	2.509	0.033	Significant
Interaction $A'C'$	0.0014	1	0.00135	2.478	0.035	Significant
Residual	0.0020	9	0.00022			
Lack of Fit	0.0018	5	0.00035	6.200	0.051	Not significant
Pure Error	0.0002	4	0.00006			
Cor Total	0.0148	16				

Based on Equations (2) and (3), sintering parameters can be optimized by looking for combinations of values of heating rate, temperature and holding time that will produce the highest density of Al_2O_3 ceramics after sintering. According to both RSM models, the highest density values of Al_2O_3 ceramics occur during longer sintering at higher temperatures. The influence of the heating rate in the examined value range from 3 °C/min to 7 °C/min has a negligible effect on the increase of the density. Therefore, the highest density of Al_2O_3 ceramics (3.893 g/cm³) can be achieved after sintering at 1625 °C for 6 h, with a heating rate of 7 °C/min.

4. Conclusions

In this investigation, highly concentrated aqueous suspensions (70 wt.%) of alumina ceramics were prepared. To stabilize them and to achieve the lowest viscosity, optimal for gravity slip casting, the optimum amount of the commercial dispersant Dolapix CE 64 was determined by rheological measurements and found to be 0.2 wt.%.

By using the Box–Behnken design of experiments and the response surface methodology the optimum working parameters were determined for pressureless sintering of alumina green castings in an air electric furnace. The heating rate of 7 °C/min, the sintering temperature of 1625 °C and the holding time of 6 h were found to be the optimum process parameters to achieve maximum density of Al_2O_3 alumina ceramics. Linear and nonlinear models with added first-order interaction were developed in terms of sintering temperature, heating rate and holding of time to represent density and the corresponding coefficients of independent variables were estimated with ANOVA analysis by the Design-Expert software. The response variable, density, evaluated from the proposed nonlinear model shows a better agreement with the results of experiments compared to the linear model. Both models gave the same optimum sintering conditions for producing a maximum density of alumina.

To improve the accuracy of the density prediction model in future research, the possibilities of application of other DOE configurations such as the centrally composite plan and the three-level factorial plan should be considered. These experimental plans provide a response surface that is a parabolic function of the analyzed factors. With

quadratic response surface the additional physical model inherent parameters related to densification kinetics and grain growth can be introduced into a nonlinear model to achieve a better fit of density changes during sintering process.

Author Contributions: Conceptualization, D.L. and L.Ć.; methodology, D.L. and L.Ć.; software, D.L. and I.Ž.; validation, L.Ć., M.K.M. and D.L.; formal analysis, I.G.; investigation, I.G.; resources, L.Ć.; data curation, D.L. and L.Ć.; writing, D.L., L.Ć., I.G. and M.K.M.; writing—review and editing, D.L., L.Ć. and I.Ž.; visualization, L.Ć. and I.G.; supervision, L.Ć. and D.L.; project administration, L.Ć.; funding acquisition, L.Ć. All authors have read and agreed to the published version of the manuscript.

Funding: This work has been fully supported by Croatian Science Foundation under the project IP-2016-06-6000: Monolithic and composite advanced ceramics for wear and corrosion protection (WECOR).

Institutional Review Board Statement: Not applicable.

Informed Consent Statement: Not applicable.

Data Availability Statement: The data presented in this study are available upon request from the corresponding author.

Conflicts of Interest: The authors declare no conflict of interest.

References

1. Yuan, C.S.; Wang, Z.J.; Zhi, Q.; Zhang, Y.M.; Wang, X.D.; Yang, J.F. The preparation and properties of alumina ceramics through a two-step pressureless sintering process. *Mater. Sci. Forum* **2018**, *922*, 47–54. [[CrossRef](#)]
2. Chen, Z.; Li, Z.; Li, J.; Liu, C.; Lao, C.; Fu, Y.; Liu, C.; Li, Y.; Wang, P.; He, Y. 3D printing of ceramics: A review. *J. Eur. Ceram. Soc.* **2019**, *39*, 661–687. [[CrossRef](#)]
3. Tsetsekou, A.; Agrafiotis, C.; Leon, I.; Miliadis, A. Optimization of the rheological properties of alumina slurries for ceramic processing applications Part II: Spray-drying. *J. Eur. Ceram. Soc.* **2001**, *21*, 493–506. [[CrossRef](#)]
4. Hotta, T.; Abe, H.; Naito, M.; Takahashi, M.; Uematsu, K.; Kato, Z. Effect of coarse particles on the strength of alumina made by slip casting. *Powder Technol.* **2005**, *149*, 106–111. [[CrossRef](#)]
5. Tallon, C.; Limacher, M.; Franks, G.V. Effect of particle size on the shaping of ceramics by slip casting. *J. Eur. Ceram. Soc.* **2010**, *30*, 2819–2826. [[CrossRef](#)]
6. Tinke, A.P.; Govoreanu, R.; Weuts, I.; Vanhoutte, K.; De Smaele, D. A review of underlying fundamentals in a wet dispersion size analysis of powders. *Powder Technol.* **2009**, *196*, 102–114. [[CrossRef](#)]
7. Zürcher, S.; Graule, T. Influence of dispersant structure on the rheological properties of highly-concentrated zirconia dispersions. *J. Eur. Ceram. Soc.* **2005**, *25*, 863–873. [[CrossRef](#)]
8. Wu, L.; Huang, Y.; Liu, L.; Meng, L. Interaction and stabilization of DMF-based alumina suspensions with citric acid. *Powder Technol.* **2010**, *203*, 477–481. [[CrossRef](#)]
9. Wu, L.; Huang, Y.; Wang, Z.; Liu, L. Interaction and dispersion stability of alumina suspension with PAA in N,N'-dimethylformamide. *J. Eur. Ceram. Soc.* **2010**, *30*, 1327–1333. [[CrossRef](#)]
10. Sarraf, H.; Havrda, J. Rheological behavior of concentrated alumina suspension: Effect of electrosteric stabilization. *Ceram. Silik.* **2007**, *51*, 147–152.
11. Khan, A.U.; Ul Haq, A.; Mahmood, N.; Ali, Z. Rheological studies of aqueous stabilised nano-zirconia particle suspensions. *Mater. Res.* **2012**, *15*, 21–26. [[CrossRef](#)]
12. Vukšić, M.; Žmak, I.; Ćurković, L.; Ćorić, D. Effect of additives on stability of alumina-waste alumina suspension for slip casting: Optimization using Box-Behnken design. *Materials* **2019**, *12*, 1738. [[CrossRef](#)]
13. Sever, I.; Zmak, I.; Ćurković, L.; Švagelj, Z. Stabilization of highly concentrated alumina suspensions with different dispersants. *Trans. Famena* **2018**, *42*, 61–70. [[CrossRef](#)]
14. Dhuban, S.B.; Ramesh, S.; Tan, C.Y.; Wong, Y.H.; Alengaram, U.J.; Teng, W.D.; Tarlochan, F.; Sutharsini, U. Sintering behaviour and properties of manganese-doped alumina. *Ceram. Int.* **2019**, *45*, 7049–7054. [[CrossRef](#)]
15. Yang, Z.; Yin, Z.; Wang, D.; Wang, H.; Song, H.; Zhao, Z.; Zhang, G.; Qing, G.; Wu, H.; Jin, H. Effects of ternary sintering aids and sintering parameters on properties of alumina ceramics based on orthogonal test method. *Mater. Chem. Phys.* **2020**, *241*, 122453. [[CrossRef](#)]
16. Ćurković, L.; Veseli, R.; Gabelica, I.; Žmak, I.; Ropuš, I.; Vukšić, M. A review of microwave-assisted sintering technique. *Trans. Famena* **2021**, *45*, 1–16. [[CrossRef](#)]
17. Curto, H.; Thuault, A.; Jean, F.; Violier, M.; Dupont, V.; Hornez, J.C.; Leriche, A. Coupling additive manufacturing and microwave sintering: A fast processing route of alumina ceramics. *J. Eur. Ceram. Soc.* **2020**, *40*, 2548–2554. [[CrossRef](#)]
18. Liu, L.; Hou, Z.; Zhang, B.; Ye, F.; Zhang, Z.; Zhou, Y. A new heating route of spark plasma sintering and its effect on alumina ceramic densification. *Mater. Sci. Eng. A* **2013**, *559*, 462–466. [[CrossRef](#)]

19. Sun, Z.; Li, B.; Hu, P.; Ding, F.; Yuan, F. Alumina ceramics with uniform grains prepared from Al₂O₃ nanospheres. *J. Alloy. Compd.* **2016**, *688*, 933–938. [[CrossRef](#)]
20. Batista, H.A.; Silva, F.N.; Lisboa, H.M.; Costa, A.C.F.M. Modeling and optimization of combustion synthesis for hydroxyapatite production. *Ceram. Int.* **2020**, *46*, 11638–11646. [[CrossRef](#)]
21. Khajelakzay, M.; Bakhshi, S.R. Optimization of spark plasma sintering parameters of Si₃N₄-SiC composite using response surface methodology (RSM). *Ceram. Int.* **2017**, *43*, 6815–6821. [[CrossRef](#)]
22. Das, S.; Madheshiya, A.; Das, S.; Gautam, S.S.; Gautam, C. Mechanical, surface morphological and multi-objective optimization of tribological properties of V₂O₅ doped lead calcium titanate borosilicate glass ceramics. *Ceram. Int.* **2020**, *46*, 19170–19180. [[CrossRef](#)]
23. Jiang, L.; Guo, S.; Bian, Y.; Zhang, M.; Ding, W. Effect of sintering temperature on mechanical properties of magnesia partially stabilized zirconia refractory. *Ceram. Int.* **2016**, *42*, 10593–10598. [[CrossRef](#)]
24. Arzani, M.; Mahdavi, H.R.; Bakhtiari, O.; Mohammadi, T. Preparation of mullite ceramic microfilter membranes using Response surface methodology based on central composite design. *Ceram. Int.* **2016**, *42*, 8155–8164. [[CrossRef](#)]
25. Kockal, N.U. Optimizing production parameters of ceramic tiles incorporating fly ash using response surface methodology. *Ceram. Int.* **2015**, *41*, 14529–14536. [[CrossRef](#)]
26. Li, J.; Peng, J.; Guo, S.; Zhang, L. Application of response surface methodology (RSM) for optimization of the sintering process of preparation calcia partially stabilized zirconia (CaO-PSZ) using natural baddeleyite. *J. Alloy. Compd.* **2013**, *574*, 504–511. [[CrossRef](#)]
27. Tarō, G.; Ferreira, J.M.F.; Lyckfeldt, O. Influence of the stabilising mechanism and solid loading on slip casting of alumina. *J. Eur. Ceram. Soc.* **1998**, *18*, 479–486. [[CrossRef](#)]
28. Rao, S.P.; Tripathy, S.S.; Raichur, A.M. Dispersion studies of sub-micron zirconia using Dolapix CE 64, Colloids and Surfaces A: Physicochem. Eng. Asp. **2007**, *302*, 553–558. [[CrossRef](#)]
29. Kang, S.J.L.; Jung, Y. Sintering kinetics at final stage sintering: Model calculation and map construction. *Acta Mater.* **2004**, *52*, 4573–4578. [[CrossRef](#)]